THE JOURNAL OF PHYSICAL CHEMISTRY Letters

Perspective

pubs.acs.org/JPCL

Electronic Delocalization, Vibrational Dynamics, and Energy Transfer in Organic Chromophores

Tammie Nelson,[†] Sebastian Fernandez-Alberti,[‡] Adrian E. Roitberg,[§] and Sergei Tretiak*[,†]

[†]Theoretical Division, Los Alamos National Laboratory, Los Alamos, New Mexico 87545, United States

[‡]Universidad Nacional de Quilmes/CONICET, Roque Saenz Peña 352, B1876BXD Bernal, Argentina

[§]Department of Chemistry, University of Florida, Gainesville, Florida 32611, United States

ABSTRACT: The efficiency of materials developed for solar energy and technological applications depends on the interplay between molecular architecture and light-induced electronic energy redistribution. The spatial localization of electronic excitations is very sensitive to molecular distortions. Vibrational nuclear motions can couple to electronic dynamics driving changes in localization. The electronic energy transfer among multiple chromophores arises from several distinct mechanisms that can give rise to experimentally measured signals. Atomistic simulations of coupled electron-vibrational dynamics can help uncover the nuclear motions directing energy flow. Through careful analysis of excited state wave function evolution and a useful fragmenting of multichromophore systems, through-bond transport and exciton hopping (through-space) mechanisms can be distinguished. Such insights are crucial in the interpretation of fluorescence anisotropy measurements and can aid materials design. This Perspective highlights the interconnected vibrational and electronic motions at the foundation of nonadiabatic dynamics where nuclear motions, including torsional rotations and bond vibrations, drive electronic transitions.

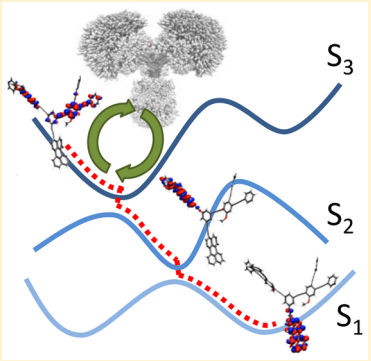

The efficient conversion of light energy into other usable forms of energy with minimal loss lies at the heart of our efforts to develop solar power as a clean energy source. Among natural organisms, the conversion of light energy, absorbed as solar radiation, into chemical energy is commonly achieved through highly efficient and complex arrays of conjugated chromophores.[1,2] The continuous development of new synthetic light harvesters that mimic natural photosynthetic complexes has produced a plethora of materials that can play the active role in organic photovoltaics, light emitting diodes, sensors, and a variety of other solar energy conversion applications. They range from supramolecular assemblies[3] and porphyrin- or bodipy-based chromophore arrays[4−7] and metal organic frameworks,[8] to macrocyclic polymers[9,10] and dendrimers[11,12] that combine several chromophores into a single giant molecule. A unifying theme among these synthetic light harvesting materials is the role of molecular architecture in determining the energy transfer dynamics that ultimately leads to energy transport and the spatial focusing of photon energy in the form of localized electronic excitations/excitons into target molecular systems. At the same time, molecular architecture can be exploited to minimize losses to heat (caused by vibrational relaxation) and losses of excitations (quenching) at defect sites. The key to designing new high efficiency materials is understanding the fundamental role of molecular architecture in guiding the electronic and vibrational dynamics and subsequent energy transfer processes.

Ideal light harvesting materials contain an inherent intramolecular energy gradient so that, following light absorption, an electronic excitation undergoes efficient and unidirectional energy funneling to lower energy sites where emission or charge separation can occur. The efficiency of energy transfer is strongly tied to the associated time scale. Ultrafast energy transfer processes tend to be highly efficient because of the significant reduction in energy loss to other degrees of freedom, such as the solvent, that would be more probable for slower processes. Within this framework, the multichromophore systems mentioned above have emerged as promising candidates due to their π-conjugated structures composed of weakly coupled individual chromophore units. By incorporating multiple chromophores that absorb light at different wavelengths, the conversion efficiency can be enhanced. As a specific example highlighted in this Perspective, dendritic macromolecules combine several chromophores within a single well-defined and controllable molecular backbone. The wide range of dendritic structures are typically comprised of covalently linked chromophores where the backbone structure and conformation gives rise to built-in energy gradients and efficient intramolecular energy funneling.[13,14] The presence of multiple equivalent chromophore units in light-harvesting materials, including dendrimers, leads to a competition between intra- and inter- chromophore energy transfer pathways and introduces a complex interplay between electronic and vibrational transfer processes.

The movement of an excitation from one chromophore unit to another can be monitored by a variety of time-resolved

Received: April 1, 2017
Accepted: June 12, 2017
Published: June 12, 2017

DOI: 10.1021/acs.jpclett.7b00790
J. Phys. Chem. Lett. 2017, 8, 3020−3031

spectroscopies, such as sophisticated 2D electronic spectroscopies[15,16] or conventional pump−probes.[17,18] For example, changes in polarization can be detected through time-resolved fluorescence anisotropy measurements. Such measurements have been used to investigate excitation localization and migration in natural[19,20] and artificial light harvesting systems including nanorings,[21] macrocycles,[9,10] and dendrimers[22] as well as conjugated polymers[23,24] and chromophore dimers.[25,26] The electronic energy redistribution among chromophore units induces a scrambling of the transition dipole orientation that can occur through several possible mechanisms. First, a delocalization of the electronic wave function can be induced by strongly coupled chromophore units or by nuclear relaxation. Alternatively, it is well-known that interactions with molecular nuclear motions or the solvent environment in conjugated polymers and dendrimers can result in changes to optical properties and stabilization of spatially localized excitations.[27] Similar sensitivity to the vibrational environment has been observed in other materials such as nanodiamonds.[28] For weakly coupled chromophores, a stochastic exciton hopping mechanism can occur between sites localized in a single unit. Exciton hopping is characterized by short-range interchromophore energy migration between adjacent localized sites (chromophores).[29,30] If geometric distortions are not sufficient to bring electronic states into resonance, then exciton hopping will be absent, and the complete relaxation can occur within a single chromophore unit. In that case, localization persists in a single unit where the choice of chromophore is randomly distributed. Regardless of the mechanism, it is clear that the vibrational dynamics and conformational disorder plays a vital role in the energy transfer dynamics, and excitation localization can be very sensitive to geometry distortions and morphology changes.[18,31−39] The variation in the strength of the nonadiabatic couplings, which modulate the interaction between the electronic and vibrational degrees of freedom, and the extent of exciton (de)localization both contribute to the final electronic distribution among different chromophore units following energy transfer.

Probing the formation, evolution, and decay of excitations in photoactive materials requires an understanding of nonadiabatic dynamics that couples electronic and nuclear motions.

Probing the formation, evolution, and decay of excitations in photoactive materials requires an understanding of nonadiabatic (NA) dynamics that couples electronic and nuclear motions. NA dynamics can lead to energy transfer during the nonradiative relaxation to the ground or low lying excited states. The modeling of nanometer length scale and subnanosecond time scale dynamics of excited electron-vibrational states can be achieved through mixed quantum-classical dynamics methods to go beyond the Born−Oppenheimer approximation. This Perspective is organized as follows: First, we present a discussion of the methodology commonly used to model NA dynamics in organic conjugated materials and the analysis of electronic transition density matrices that can be used to track changes in spatial localization resulting from energy transfer. Next, we present examples of the effect of conformational disorder and coupling of electronic and nuclear motions on energy transfer dynamics. We demonstrate these effects by analyzing nuclear motions in nanohoops, specifically the torsional modes, that contribute to exciton trapping. Finally, we consider the interpretation of energy transfer mechanisms appearing in fluorescence depolarization.

Nonadiabatic Excited-State Molecular Dynamics. Modeling dynamics on multiple coupled electronic states through regions of strong nonadiabatic coupling can be performed using mixed quantum classical trajectory surface hopping approaches.[40] Generally, these methods rely on a classical treatment of nuclei and a quantum mechanical description of electrons, which evolve through the time-dependent Schrödinger equation (TDSE) or Von Neumann equation with various prescriptions for computing transition probabilities between coupled electronic states. Numerous formulations of surface-hopping-based simulations have been developed over the years to model large molecular systems and can include decoherence effects and spin−orbit coupling,[41−50] as well as quantum mechanics/molecular mechanics (QM/MM) methods for protein and solution environments.[51] Popular among these methods is the fewest switches surface hopping (FSSH) approach,[52] where transitions between coupled electronic states describe the feedback between the electronic system and nuclear motions, and the probability of changing the active potential energy surface (PES) is calculated based on the strength of the nonadiabatic coupling. Energy transfer between states commonly takes place through the direction defined by the nonadiabatic coupling vector (NACR), which is related to specific excited state normal modes.[53,54] The direction of NACR can be interpreted as the nonadiabatic contribution to the direction of the main driving force on the nuclei during electronic transitions, and the strength of the nonadiabatic coupling can be strongly affected by the effective nuclear velocities in the direction of the nonadiabatic coupling vector. Furthermore, normal modes that actively participate in the electronic relaxation processes are characterized by the highest overlap with the nonadiabatic coupling vectors during the electronic transitions, as demonstrated, for example, in chlorophyll A,[55] confirming the relevance of the NACR direction during energy transfer.

The nonadiabatic excited-state molecular dynamics (NA-ESMD) methodology developed by our group incorporates quantum transitions among excited states using the FSSH scheme. Following photoexcitation, the electronic wavefunction evolves through the TDSE, while nuclei evolve according to Newton's equation or constant-temperature Langevin dynamics[56,57] with forces from the excited state PES. The simulations of coupled nuclear and electronic dynamics must use the true PESs and forces in the excited states. This goes well beyond the commonly used classical path approximation (CPA), where a single trajectory and only the ground state PES is used. True PESs are crucial for capturing the changes in forces between electronic surfaces that promote localization/delocalization and energy transfer. The collective electronic oscillator (CEO) approach[58,59] is used to compute electronic excited states at the configuration interaction singles (CIS) level of theory with a semiempirical Hamiltonian.[60,61] Many independent trajectories are required to generate a statistical ensemble where the population of each quantum state is given by the fraction of trajectories on each PES. Observables such as excited-state lifetimes and energy transfer rates are averages over the ensemble of trajectories, and the fluorescence anisotropy can be

DOI: 10.1021/acs.jpclett.7b00790
J. Phys. Chem. Lett. 2017, 8, 3020−3031

directly modeled,[62,63] providing a level of mechanistic detail beyond what can be achieved through experiment alone. A detailed description of the NA-ESMD methodology can be found elsewhere.[64−68] These simulations have made it possible to successfully describe photoinduced processes in a variety of extended molecular systems.[18,37,38,53,62,69−72]

Implementation of hybrid quantum-classical methods, like FSSH, in extended conjugated molecules composed of sets of individual chromophores required a test of parameters and approximations previously proposed for model molecules.[65] It has been found that many previously suggested simplifications fail for realistic molecules with dense manifold of excited states, hundreds of vibrational degrees of freedom, and strongly varying vibrational frequencies and electron−phonon coupling constants.[65,67] For example, including NA couplings of states not directly involved in the internal conversion process can have a significant impact on the electronic relaxation rates.[65] Other simplifications that are not required in model systems, such as "on-the-fly" state limiting, have significantly reduced the computational costs for large systems.[73]

Additional considerations for modeling multichromophore molecules must be included in FSSH-based simulations to overcome its various limitations.[43] For spatially separated noninteracting electronic states brought into resonance by nuclear motions, we developed a state tracking algorithm[66,74] to distinguish between unavoided crossings involving interacting states (simulated by quantum hops) and trivial unavoided crossings between noninteracting states (detected by state tracking). Other solutions for the trivial crossing problem have been proposed.[75−77] In addition, several sophisticated approaches for incorporating decoherence in trajectory surface hopping simulations have also been developed over the years.[44,77−80] In recent years, there has been a renewed interest in deriving formally exact surface hopping approaches.[81−83] In particular, dynamical methods based on the propagation of Gaussian wavepackets, such as the widely used ab initio multiple spawning (AIMS) method[84] and others,[42,85,86] provide a fully ab initio description of quantum coherence effects. Despite their success, applications to large molecular systems (100s of atoms) are still typically too expensive. The NA-ESMD employs instantaneous decoherence[67] by resetting quantum amplitudes after a hop.

The NA-ESMD simulations presented in the following sections have been performed within the basis of adiabatic states. However, geometrical distortions can affect the energy ordering of the corresponding diabatic states, leading to a change in the electronic character and/or label of the adiabatic state. Therefore, it is more convenient to understand results in terms of diabatic states defined according to their electronic character. For clarity, we define the state labels used throughout the remainder of the discussion: S_n refers to the diabatic state where n refers to the initial energy ordering at time $t = 0$.

Electronic Transition Densities. The transition density (TD) matrices compactly reflect the properties of many-body wave functions and provide a simplified picture of wave function dynamics. Subsequently, these are convenient quantities to analyze energy transfer occurring through a change in the spatial excitation localization. Energy transfer and the extent of (de)localization can be followed in the NA-ESMD simulations through the spatial localization of the electronic TD. Transition density matrices are calculated within the CEO formalism[58,59] as $(\rho^{0\alpha})_{nm}=\langle\phi_\alpha(r;\mathbf{R}(t))|c_m^+c_n|\phi_0(r;\mathbf{R}(t))\rangle$ where $\phi_0(r;\mathbf{R}(t))$ and $\phi_\alpha(r;\mathbf{R}(t))$ are the ground and excited state CIS adiabatic wave functions, respectively. n and m represent atomic orbital (AO) basis functions, and c_m^+ and c_n are creation and annihilation operators. The diagonal elements $(\rho^{0\alpha})_{nn}$ represent the net change in the electronic density distribution for a ground to excited state transition. In contrast, the off-diagonal elements of $(\rho^{0\alpha})_{nm}$ describe electronic coherences and charge-transfer phenomena.[87,88] Subsequently, the orbital representation of these quantities is beneficial for the analysis of a variety of excited state properties. For example, natural transition orbitals (NTOs) developed by Martin[89] express the electronic transition density matrix as essential pairs of particle and hole orbitals, thus enabling examination of electron−hole separation in excitonic wave functions and charge-transfer states. Furthermore, the orbital representation of the diagonal elements is convenient to analyze the total spatial extent of the excited state wave function,[68] which is extensively used in this work. The normalization condition $\sum_{n,m}(\rho^{0\alpha})_{nm}^2 = 1$ applies within the CIS approximation[90] owing to the fact that transition density matrices are normalized eigenvectors of the CIS operator. In multichromophore systems, it is convenient to partition the molecular system into chromophore fragments allowing the fraction of the transition density (δ_X^α) localized on each chromophore unit X to be found by summing the contributions from each atom (index A) in X given by $\delta_X^\alpha = (\rho^{0\alpha})_X^2 = \sum_{n_A m_A}(\rho^{0\alpha})_{n_A m_A}^2$.

While transition densities describe electronic systems, the evolution of vibrational degrees of freedom is reflected in nuclear motions.

Analysis of Vibrational Dynamics. While the transition densities describe the electronic system, the evolution of vibrational degrees of freedom is reflected in nuclear motions. Since it is impossible to follow all vibrational degrees of freedom, even for a small molecule, the nuclear motions that are strongly coupled to the electronic degrees of freedom serve as a convenient vibrational descriptor. In particular, bond length alternation (BLA) and torsions (dihedral angles) represent the fast and slow nuclear coordinates, respectively, common in soft conjugated organic materials.[64,91] The BLA gives the average difference between the single (C−C) and double (C═C) bond lengths of a vinylene segment and is defined by $[\{(d_1 + d_3)/2\} - d_2]$, where d_1 and d_3 are the lengths of single bonds, and d_2 is the length of the double bond.

Conformational Disorder. The ubiquitous soft molecular structure among organic conjugated polymers and chromophores leaves their molecular geometry highly susceptible to thermal fluctuations. These thermally induced geometry variations produce the effect commonly known as conformational disorder. The conformational variation of the backbone geometry in organic conjugated materials, including dendrimers, impacts the electronic transition density localization and thus the relative balance between intra- and interchromophore energy transfer and the available through-space and sequential through-bond energy transfer mechanisms. The accessible space of the conformational landscape can be strongly influenced through thermal fluctuations and depends on steric interactions between units. The effect of conforma-

DOI: 10.1021/acs.jpclett.7b00790
J. Phys. Chem. Lett. 2017, 8, 3020−3031

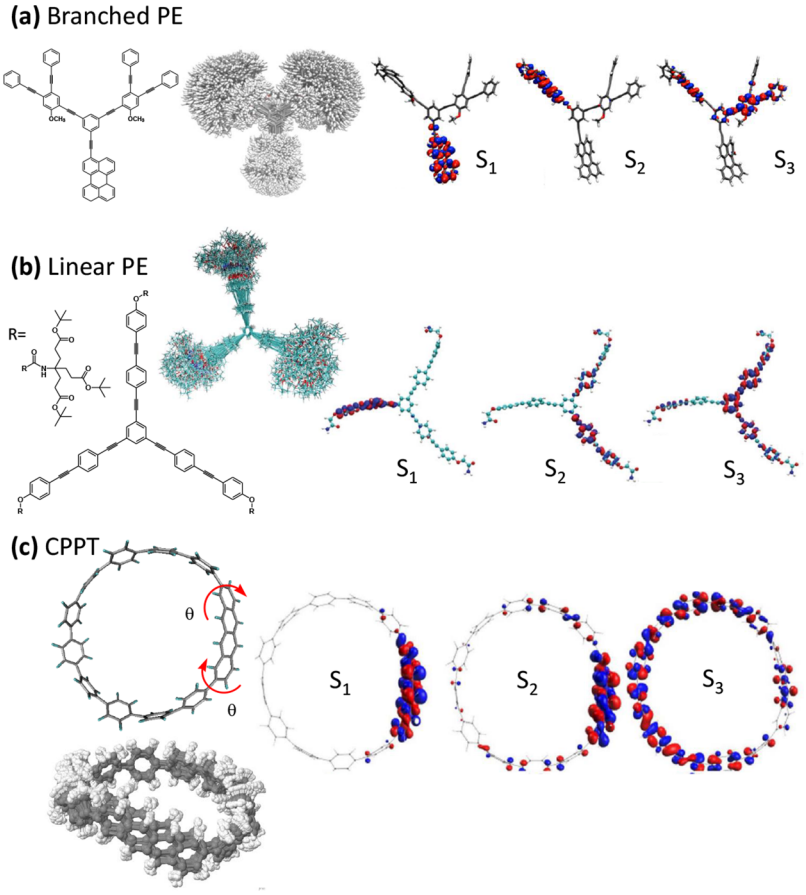

Figure 1. (a) Chemical structure of branched phenylene-ethynylene (PE) dendrimer and ground-state conformational disorder of 1000 configurations. The electronic transition density localization for the three lowest energy electronic excited states indicates energy funneling to a perylene sink in S_1. (b) Chemical structure of linear PE dendrimer and ground-state conformational disorder of 400 configurations. The electronic transition density localization for the three lowest energy electronic excited states suggest exciton trapping in a single branch in S_1. (c) Chemical structure of the nanohoop composed of cyclo para-phenylene with an inserted tetracene unit (CPPT) with large strain-induced dihedral angles around the tetracene defect and the resulting conformational disorder among 750 configurations. The electronic transition density localization for the three lowest energy electronic excited states indicates energy transfer to the tetracene insertion in S_1.

tional variation on the electronic TD localization is demonstrated in Figure 1 for different molecular architectures.

The branched phenylene-ethynylene (PE) dendrimer[18] with ortho, meta, and para linked units and an ethynylene-perylene (EPer) energy sink shown in Figure 1a demonstrates conformational disorder in the ground-state sampling of 1000 configurations. The orbital representation of the electronic TD reveals an intramolecular energy gradient leading to fast energy funneling to the sink. The changes in localization during nonradiative relaxation leads to exciton trapping in the EPer sink: $S_{\geq 3}$ states are delocalized over both PE fragments, the S_2 state is localized in one PE unit, and S_1 is localized in the EPer sink. Alternatively, the chemical structure of a PE dendrimer with three equivalent linear PE units attached with meta branching[37] in shown in Figure 1b. Dendrimers with chromophores of the same conjugation length lack an energy gradient. The superposition of molecular geometries obtained from the ground-state QM/MM conformational sampling in THF solvent reveals the conformational disorder. Despite the absence of an energy gradient, the meta branching breaks the conjugation leading to localized excitations: the transition density of S_1 is mostly localized in one PE branch, with S_2 and S_3 states delocalized between the two other branches. Finally, we consider the chemical structure of the cyclo para-phenylene (CPP) presented in Figure 1c. The nanohoop is composed of 10 phenyl units with an inserted tetracene defect (CPPT).[70] The defect introduces strain in the hoop and large dihedral angles produce geometric variations among the 750 depicted ground-state configurations. In general, temperature-induced conformational disorder in CPP systems leads to wider torsional distributions, breaking the π-conjugation. This symmetry breaking is more pronounced for large acenes leading to state localization and exciton trapping. The S_1 and S_2 states of CPPT have TD strongly localized in the tetracene unit while S_3 is delocalized.

Conformational fluctuations can occur simultaneously with electronic relaxation, making the energy transfer a dynamical process rather than a static one.[35] Nuclear motions along a dendrimer or polymer backbone can create quasi-degeneracy, resulting in ultrafast changes to exciton localization, while, at the same time, the electronic relaxation takes place between states whose electronic character and localization are changing. It is important to stress that energy transfer in systems composed of chromophores of similar conjugation length can rarely be described by a single well-defined pathway due to conformational variety involving multiple chromophore units.[24,36] In light harvesting complexes composed of multiple chromophores, the energy transfer involves excitations

DOI: 10.1021/acs.jpclett.7b00790
J. Phys. Chem. Lett. 2017, 8, 3020−3031

delocalized over multiple chromophores. As long as the donor and acceptor sites are well separated in space, a rate description based on Förster theory can be applied. However, conformational disorder can introduce kinks in the backbone of the polymer to break the conjugation, which can significantly impact the rate of excitation energy migration and electronic relaxation. This has been experimentally confirmed, for example, by photoluminescence anisotropy decay in PPV-family conjugated polymers[24] and porphyrin nanorings.[92] As a consequence, such kinks can lead to excited state energy reordering and reverse directions of energy transfer,[36] overlap between the absorbance of donor and acceptor units, interference between multiple pathways,[63] and complex rates that cannot be adequately described by a Förster model based on a single rate.

Conformational disorder can introduce kinks in the backbone of the polymer to break the conjugation, which can significantly impact the rate of excitation energy migration and electronic relaxation.

Electron-Vibrational Coupling Effects. Let us consider more closely the energy transfer in the branched PE dendrimer of Figure 1a to demonstrate that changes in localization are coupled to nuclear motions. Photoexcitation of the branched PE dendrimer creates a delocalized excited state spanning both PE units ($S_{\geq 3}$) due to the high density of excited states (Frenkel excitons) and the thermal fluctuations producing a variety of initial conformations (see Figure 1a). During the nonradiative relaxation, nonadiabatic transitions are driven by strong coupling to high-frequency vibrational modes, causing the excitation to quickly collapse to a more localized intermediate state S_2 in a single PE branch before finally reaching the EPer sink in S_1.

Adiabatic vibrational relaxation of the lowest energy excited state has been implicated in self-trapping of excitons through strong coupling to torsional and C−C nuclear motions; however, in this case, the localization occurs on an ultrafast (subpicosecond) time scale. The change in the transition density localization in the branched PE dendrimer around the $S_3 \rightarrow S_2$ transition is revealed in the contour plot in Figure 2a. The blue-green color scale indicates the transition density of the PE unit with the higher TD contribution (labeled H), and the red-yellow color scale corresponds to the other PE unit with the lower contribution (labeled L). During the $S_3 \rightarrow S_2$ transition, the electronic energy is located in the backbone with negligible contribution from the EPer sink. The transition occurs at $\Delta t = 0$. For $\Delta t < 0$ the system is in the S_3 state, and the TD is delocalized over both PE units. After the transition, at $\Delta t > 0$, the system is in S_2 and the contour distribution shows the contribution of the L unit drops to almost 0, while most of the TD is localized in the H unit, indicating that it becomes localized on a single PE unit through coupling with the nuclear dynamics. Similarly, the $S_2 \rightarrow S_1$ transition corresponds to the backbone-to-trap energy transfer, and the contour plot of the transition density associated with this transition is shown in Figure 2b. At the time of the nonadiabatic transition, the TD changes from being localized in a single PE unit (blue) to being fully localized in the EPer trap (red). This example highlights the effect of electronic and vibrational coupling. The changes in localization both within the PE branches and between the PE units and the EPer trap are concomitant with the strong nonadiabatic coupling represented by the $S_3 \rightarrow S_2$ and $S_2 \rightarrow S_1$ transitions, respectively. That is a clear indication that the changes in localization are directly coupled to the nuclear motions.

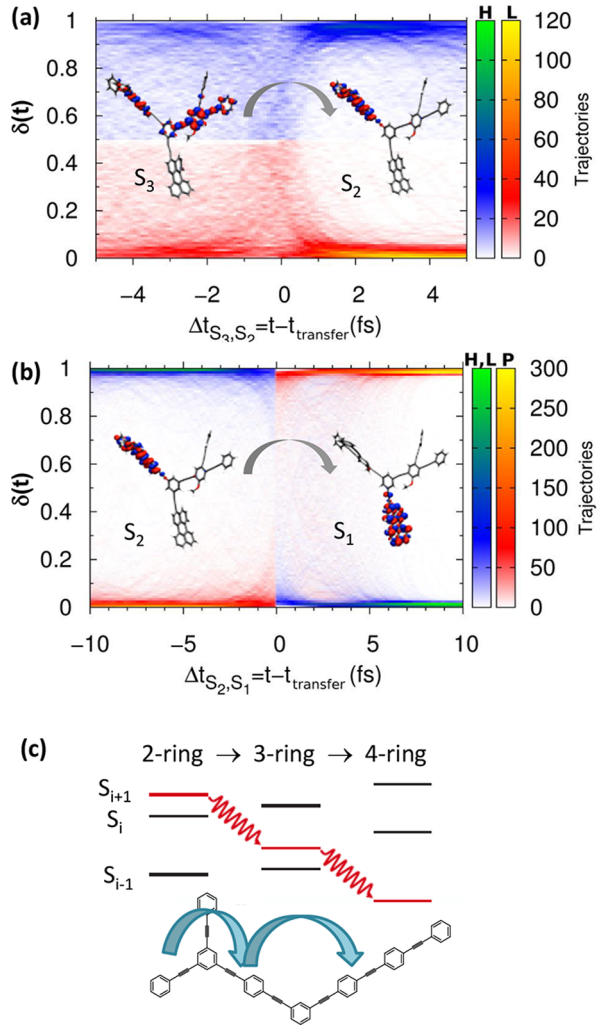

Figure 2. (a) Contour plot of the transition density composition before and after the $S_3 \rightarrow S_2$ (delocalized PE state to localized PE state) transition. The blue-green color scale represents the PE unit with higher TD contribution (H) and the red-yellow color scale represents the PE unit with lower TD contribution (L). (b) Contour plot of the transition density composition before and after the $S_2 \rightarrow S_1$ (localized PE state to localized trap state) transition. The blue-green color scale represents the PE units, while the red-yellow color scale represents the perylene trap (P). (c) Jablonski diagram depicting the unidirectional energy transfer mechanism that takes place due to differential nuclear motions in a model PE dendrimer.

The coupling between vibrational motions and energy transfer is clearly evident in the PE dendrimer shown in Figure 2c. In this system, energy transfer is induced by differential nuclear motion on the PESs modulating the energy difference between states and enforcing the unidirectional downhill mechanism.[69] While the electronic population is mostly on S_{i+1} (localized in the 2-ring units), nuclear motions on the S_{i+1} surface keep the energy gap between S_{i+1} and S_i small. This

DOI: 10.1021/acs.jpclett.7b00790
J. Phys. Chem. Lett. 2017, 8, 3020−3031

favors the energy transfer between them since the nonadiabatic couplings are inversely proportional to the energy difference.[93] After the electronic population is transferred to S_i (localized on the 3-ring unit), the nuclear motion on S_i decouples S_i and S_{i+1} but starts to couple S_i with S_{i-1}. The energy transfer between these new states persists until most of the population has been transferred to S_{i-1} (localized in the 4-ring unit). It has been demonstrated that the triple bond excitations coincide with the localization of the electronic transition densities, meaning that the energy transfer dynamics is a concerted electronic and vibrational energy transfer process. This effect is captured in simulation by using the "native" excited state forces which differ on each surface and promote vibrational relaxation toward the excited state energy minimum. The efficient energy funneling is also observed in light harvesting donor−bridge−acceptor systems.[94,95]

Distinguishing Energy Transfer Mechanisms. The redistribution of transition density among equivalent chromophore units leads to a scrambling of the transition dipole orientation. As mentioned previously, for identical chromophore units, there can be several mechanisms that can produce scrambling, depending on how strongly chromophore units are coupled. Strong coupling produces a true delocalization of the wave function over multiple units. In the weak coupling regime, the wave function maintains its localized nature in an individual unit but either spatially migrates from unit to unit or relaxes completely within a single unit where the choice of unit is distributed among the identical chromophores.

For identical chromophore units, there can be several mechanisms that can produce scrambling, depending on how strongly chromophore units are coupled.

These mechanisms cannot always be distinguished from the changes in the ensemble-averaged TD localization. For instance, in the linear PE dendrimer composed of three equivalent units, the initial excitation is broadly distributed between two branches while the third branch is not excited. The evolution of the ensemble-averaged transition density in Figure 3a shows an equivalent final energy redistribution among all three chromophore units. That distribution can be achieved if all of the members of the ensemble have the excitation delocalized over all three units or if excitations are localized in a single branch with one-third of the ensemble having the localization on the three different branches. In this case, a close inspection of the transition density distributions is required and reveals that the ensemble distribution has one-third of the configurations with transition density localized in any given unit, and the choice of the unit is randomly distributed.

A similar result has been observed in dimers of organic conjugated chromophores where both coherent wave-like exciton motion and incoherent hopping mechanisms have been observed in various dimer systems.[26,96−98] For example, in dithia-anthracenophane (DTA), a sulfur connected dimer of two identical anthracene units that localize excitations, previous experimental and theoretical investigations supported a coherent resonance energy transfer mechanism.[25,99,100] However, NA-ESMD simulations of DTA[62] revealed that the

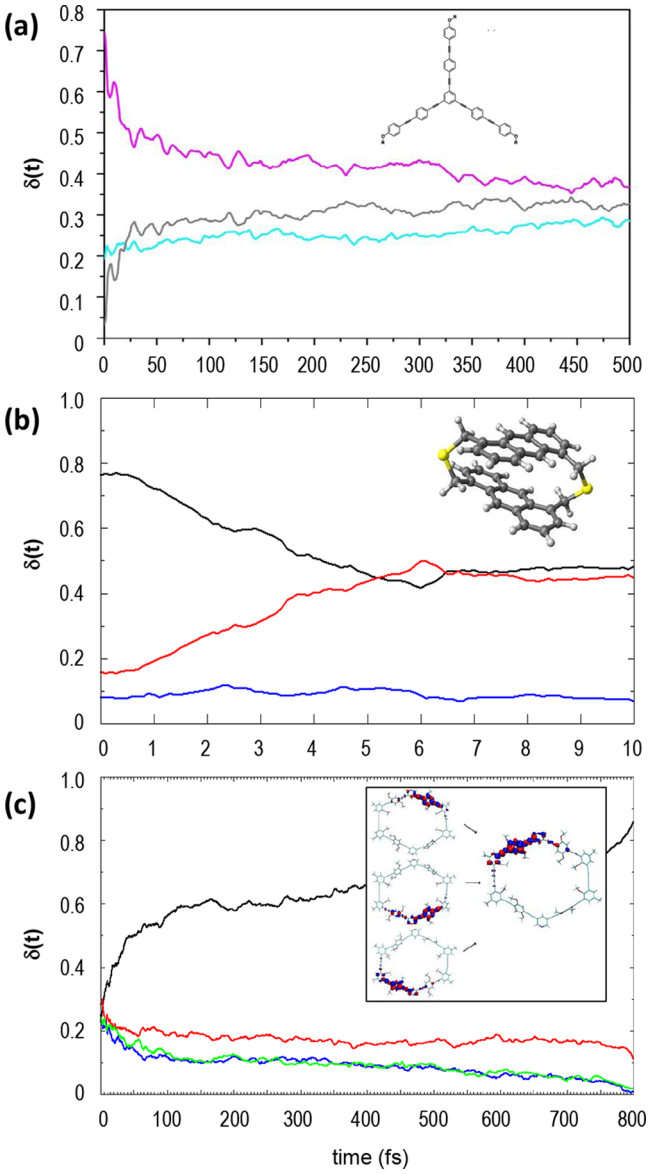

Figure 3. Evolution of the ensemble-averaged fraction of electronic transition density contained in individual chromophore units for (a) Three chromophore branches in the linear PE dendrimer, (b) two anthracene chromophores in a DTA dimer (red and black) and connecting sulfur atoms (blue), and (c) four chromophores in the PE macrocycle.

ensemble-averaged TD exchange, shown in Figure 3(b), is due to interchromophore exciton hopping between localized sites. In this case, half of the trajectories finish completely localized on one unit while the other half become fully localized on the other unit. The initial nonadiabatic coupling between states leads to an ultrafast exchange of energy between monomers while thermally induced geometric distortions and vibrational relaxation lead to localized electronic states. Ultimately, the initial confinement of the spatial excitation due to energy transfer during electronic relaxation is followed by interbranch energy transfer, while the system remains in S_1 corresponding to hopping between localized transition densities.

Finally, we compare the result of the ensemble-averaged transition density evolution in the linear PE dendrimer and DTA bichromophore, which cannot be distinguished from a true delocalization of the wave function, to the evolution in a

DOI: 10.1021/acs.jpclett.7b00790
J. Phys. Chem. Lett. 2017, 8, 3020−3031

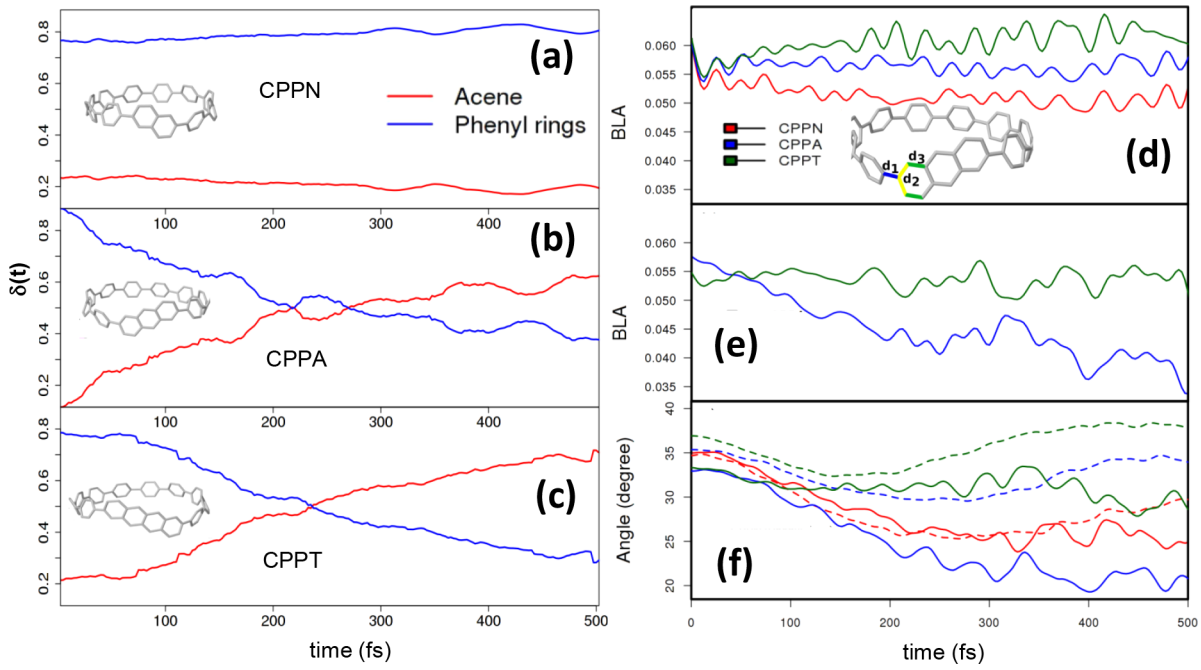

Figure 4. Time-dependent average fraction of transition density localized on the acene (red) and phenyl (blue) rings for (a) naphthalene (CPPN), (b) anthracene (CPPA), and (c) tetracene (CPPT). Evolution of the relevant vibrational motions for CPPN (red), CPPA (blue), and CPPT (green), including (d) the average bond length alternation (BLA) between phenyls, (e) the average BLA at the acene-phenylene junction, and (f) the average dihedral angles between phenyl rings (dashes) and at the acene−phenylene junction (solid).

PE macrocycle having a final localization within a single chromophore without subsequent changes in localization, just as the linear PE dendrimer. However, unlike the previous systems, Figure 3c shows an ensemble-averaged transition density evolution in the macrocycle clearly revealing the rise in localization within a single unit at the expense of the others. The ambiguity is overcome in the macrocycle because of the different choice of assignment used for tracking the units. In the linear PE dendrimer and DTA, units are assigned based on the *initial* localization of the electronic transition density. Based on that assignment, one can clearly distinguish the loss of the initially localized state, but the character of the final state is ambiguous. Instead, the four units of the PE macrocycle are assigned based on the *final* localization allowing the character of the final state to be distinguished.

The existence of multiple energy transfer pathways introduces another layer of complexity that can be solved using transition density flux methods[63] that allow the transition density exchange between specific units to be monitored. It is also possible to distinguish between inter- and intrachromophore relaxation channels by following the overlap between the current and final transition densities.[38]

Strain-Induced Geometric Distortions. Conjugated carbon nanohoops are an intriguing class of materials with unique optical properties[101] that combine strain, conformational disorder, and steric hindrance in unique ways that give rise to variations in the extent of conjugation within the molecular structure. These compounds have recently become popular candidates for light-harvesting applications and reveal a fascinating interplay between molecular distortions, delocalization and energy transfer.[10,102−104] For example, the redistribution of electronic energy in the acene-substituted CPPs[70] is strongly affected by the extent of geometric distortions introduced by the acene.

Figure 4a−c follows the changes in the electronic transition density localization in the phenyl rings and the acene unit for three different defect sizes: 2-rings (napthalene), 3-rings (anthracene), and 4-rings (tetracene). Following excitation to an initially delocalized state spanning the phenyl rings, the excitation remains delocalized around the phenyl rings for the smallest acene substitution, napthalene (CPPN; Figure 4a). In contrast, the excitation undergoes an ultrafast migration to the larger acenes. In anthracene (CPPA), the final transition density shown in Figure 4b is partially delocalized throughout the nanohoop and the anthracene. The energy transfer is most effective in tetracene (CPPT), as seen in Figure 4c, where the final excitation is concentrated on the tetracene unit. The larger acenes introduce higher strain-induced geometric distortions that break the conjugation leading to localized states.

The torsions (dihedral angles) and bond-length alternations (BLAs), plotted in Figure 4d−f, represent relevant vibrational motions that receive electronic energy during the nonradiative relaxation. π-Conjugation tends to reduce the BLA values. The BLA between phenyl rings, Figure 4d, experiences an ultrafast reduction in all three systems, which persists for CPPN, reflecting the exciton delocalization that distorts the molecular geometry. In CPPT, the initial large ground-state BLA value is recovered, and CPPA experiences a partial recovery producing the partial exciton delocalization between the phenyl units and anthracene. The BLA at the acene−phenylene junction (Figure 4e) undergoes a significant reduction for anthracene but not for tetracene, reflecting the larger extent of localization in tetracene. Smaller values of BLA at the anthracene−phenylene junction are associated with a higher degree of π-conjugation and exciton delocalization across the acene defect in CPPA. In CPPT, the large BLA value inhibits π-conjugation and leads to localization. The dihedral angles presented in Figure 4f for the acene−phenylene junction (solid) and phenyl−phenyl torsions (dashed) show a similar trend with the larger reduction moving

DOI: 10.1021/acs.jpclett.7b00790
J. Phys. Chem. Lett. 2017, 8, 3020−3031

from CPPT to CPPA to CPPN where the larger dihedral angles are associated with reduction of π-conjugation and stronger localization.

The substituted CPP nanohoops exemplify the connection between intramolecular exciton dynamics, energy transfer, and strain-induced nuclear motions in the electronic relaxation process. Similar connections have been observed in quantum dots where atomic fluctuations can lift degeneracy to overcome phonon bottlenecks in favor of fast relaxation.[105] Light harvesting within nanohoops is a complex process involving changes in localization controlled by intermediate electronic states and structural rearrangements, involving bond lengths and torsion angles, that promote electronic energy redistribution.

Fluorescence Anisotropy. The fluorescence anisotropy is often measured in experiment to detect changes in exciton localization during photodynamics by detecting changes in the transition dipole moment polarization caused by an excitation moving from one chromophore to another. The depolarization arises from the scrambling of the transition dipole orientation caused by either exciton hopping between equivalent sites or delcoalization of the wave function among different units. The fluorescence anisotropy provides an important observable, allowing computational results to be directly connected with experimental measurement. In this case, the simulated fluorescence anisotropy can help decipher which mechanisms contribute to depolarization. The fluorescence anisotropy is calculated by the expression $C(t) = \frac{2}{5}\langle P_2\{\vec{\mu}_A(0)\cdot\vec{\mu}_E(t)\}\rangle$ to give the time correlation function of the absorption dipole moment of the chromophore at time zero, $\vec{\mu}_A(t=0)$, and its emission dipole moment at time t, $\vec{\mu}_E(t)$, where $P_2(x) = \frac{1}{2}(3x^2 - 1)$ is the second-order Legendre polynomial, x is the cosine of the angle between the excitation and emission dipole moments, and the angular brackets indicate the average over all NA-ESMD trajectories.

> Fluorescence anisotropy provides an important observable, allowing computational results to be directly connected with experimental measurement.

The final ensemble in linear PE corresponds to the random distribution of excitons trapped on different PE units, where there is a similar probability of each fragment retaining a significant contribution of the transition density. The spatial redistribution among the equivalent units results from the absence of an energy gradient. The experimental fluorescence anisotropy decay in the linear PE system observed in Figure 5a in black dots can be attributed to the confinement of the electronic wave function in a single branch and hopping between the branches rather than to its expansion over the whole dendrimer. In complexes that exhibit both relaxation within a single monomer unit and exciton hopping between localized units, the fluorescence depolarization is due to both the change in localization among different monomers and the changing emission dipole orientation within a single unit. Analyzing the fluorescence anisotropy signal from a single chromophore unit can reveal what extent of the depolarization arises from each mechanism. In the case of DTA, the simulated

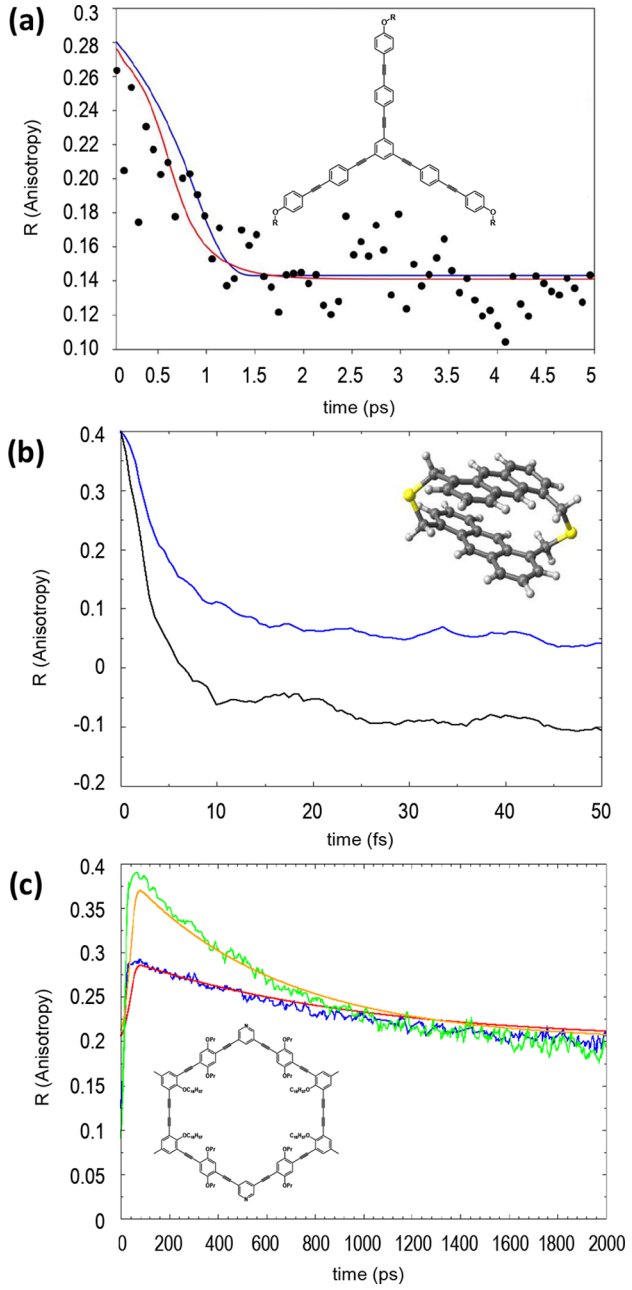

Figure 5. Examples of fluorescence anisotropy curves. (a) Simulated anisotropy decay curves for the linear PE dendrimer (blue) compared with experimental data (black) (fitting in red). (b) Simulated anisotropy decay for a single dimethyl anthracene (DMA) chromophore (blue) compared to the dithia-anthracenophane (DTA) dimer (black). (c) Simulated anisotropy decay for the PE macrocycle (red) and the half ring (orange) compared with experimental data (blue and green, respectively).

fluorescence anisotropy curves of the monomer dimethyl anthracene (DMA) and the DTA dimer are plotted in Figure 5b. The curve for DMA represents the exciton relaxation confined to a single unit. Therefore, the additional depolarization in DTA compared to DMA results from the change in localization associated with energy transfer between the rotated monomers. Similarly, Figure 5c shows the experimental and simulated depolarization curves for the PE macrocycle compared to the half ring. The macrocycle undergoes multiple energy transfer pathways from each unit to a single acceptor

DOI: 10.1021/acs.jpclett.7b00790
J. Phys. Chem. Lett. 2017, 8, 3020−3031

unit. Compared to the half ring, where energy transfer only occurs between two PE units, the additional depolarization in the macrocycle results from the interference of several pathways.

Concluding Remarks. The coupling between electronic and nuclear motions defined by nonadiabatic dynamics characterizes the formation, evolution, and decay of excitations in photoactive materials. The modeling of such complex dynamics can be achieved with semiclassical surface hopping-based approaches to go beyond the Born−Oppenheimer approximation. Sophisticated atomistic modeling in the subnanosecond regime allows information such as absorption and emission spectra, relaxation time scales, and excited state lifetimes to be accurately predicted but also reveals more complicated exciton migration pathways and mechanisms. Such simulations can provide intricate details into the vibrational motions driving the concomitant electronic transitions that ultimately lead to changes in localization associated with energy transfer. Within the nonadiabatic excited state molecular dynamics formulation, the transition density matrices describe the photoinduced spatial changes in localization that accompany energy transfer allowing multichromophore systems to be partitioned into contributions from individual fragments. The changes in localization are directly coupled to high-frequency nuclear motions that drive the nonadiabtic transitions. Specific motions involving bond lengths and torsion angles can be enhanced by strain to break conjugation and promote electronic energy redistribution and exciton trapping.

Conformational sampling diversity, which is strongly influenced by thermal fluctuations to produce a variety of initial conditions, affect the electronic transition density localization and available energy transfer pathways. Nuclear motions along polymer or dendrimer backbones can cause kinks that break conjugation and/or bring excited states localized on different chromophore units into resonance allowing ultrafast flow of energy between them. This disorder makes it almost impossible to apply the Förster model, which cannot adequately describe multiple complex rates caused by energy reordering and interference among competing pathways. Furthermore, the presence of identical chromophores makes it difficult to distinguish between possible mechanisms that result in the spatial scrambling of the transition dipole orientation. In such cases, the ambiguity can be overcome by choosing the assignment of chromophore fragments based on the initial or final localization or through the statistical minimum flow method to track energy flow between units.

The effects we have demonstrated here relate to long-lived coherence phenomena observed in multiple materials via sophisticated spectroscopies.[106] Here, they clearly result from a *vibrational* signature modulating the electronic states and bringing them into resonance. We suggest that focusing the attention on the specific role vibrational dynamics plays in guiding electronic dynamics can provide a deeper understanding of existing problems in photochemistry, photobiology, and the tailor design of photoactive materials. The insights gained from modeling will provide new interpretations of experimental measurements, such as fluorescence anisotropy decay and transient absorption spectroscopy, based on the particular combination of photophysical processes and competing mechanisms.

AUTHOR INFORMATION

Corresponding Author

*E-mail: serg@lanl.gov.

ORCID

Tammie Nelson: 0000-0002-3173-5291
Adrian E. Roitberg: 0000-0003-3963-8784
Sergei Tretiak: 0000-0001-5547-3647

Notes

The authors declare no competing financial interest.

Biographies

Dr. Tammie Nelson is a Staff Scientist at Los Alamos National Laboratory. She received her undergraduate degree from California Polytechnic State University (San Luis Obispo) in 2008 and her Ph.D. (2013) in Chemistry from the University of Rochester, NY. Her research interests include the development of efficient methods for modeling photoinduced processes in realistic molecular systems and the application of nonadiabatic excited state molecular dynamics to photochemistry in nanomaterials.

Dr. Sebastian Fernandez Alberti is a Full Professor at National University of Quilmes (UNQ, Argentina) and Independent Researcher at the National Council for Scientific and Technical Research (CONICET, Argentina). He received his undergraduate degree in 1993 from the National University of La Plata (UNLP, Argentina) and his Ph.D. in Molecular Physics in 1999 from the University of Paul Sabatier (Toulouse, France). His research interests include excited-state nonadiabatic dynamics simulations in extended conjugated molecules, electronic and vibrational relaxation, intramolecular energy redistribution in polyatomic molecules, and protein dynamics analysis using collective coordinates.

Dr. Adrian E. Roitberg is a Full Professor in the Chemistry Department at the University of Florida. He received his undergraduate degree from the University of Buenos Aires, Argentina, in 1987, and his Ph.D. from the University of Illinois at Chicago in 1992. He joined the University of Florida in 2001. His research interests are molecular modeling of molecules and materials, and studying the effect of dynamics and conformational diversity of experimental observables.

Dr. Sergei Tretiak is a Staff Scientist at Los Alamos National Laboratory. He received his M.Sc. degree from Moscow Institute of Physics and Technology (Russia) and his Ph.D. degree in 1998 from the University of Rochester. Since 2006 Tretiak has been a member of the DOE funded Center for Integrated Nanotechnologies (CINT). He also serves as an Adjunct Professor at the University of California, Santa Barbara (2015−present) and at Skolkovo Institute of Science and Technology, Moscow, Russia (2013−present). His research interests include development of modern computational methods for molecular optical properties, nonlinear optical response of organic chromophores, adiabatic and nonadiabatic molecular dynamics of excited states, optical response of confined excitons in conjugated polymers, carbon nanotubes, semiconductor nanoparticles, halide perovskites, and molecular aggregates.

ACKNOWLEDGMENTS

S.F.A. is supported by CONICET, UNQ, ANPCyT (PICT-2014-2662). S.T. and T.N. acknowledge support from Los Alamos National Laboratory (LANL) Directed Research and Development Funds (LDRD). This research used resources provided by the Los Alamos National Laboratory Institutional Computing (IC) Program, which is supported by the U.S. Department of Energy National Nuclear Security Administration. Los Alamos National Laboratory is operated by Los

DOI: 10.1021/acs.jpclett.7b00790
J. Phys. Chem. Lett. 2017, 8, 3020−3031

Alamos National Security, LLC, for the National Nuclear Security Administration of the U.S. Department of Energy under contract DE-AC52-06NA25396. We acknowledge support of the Center for Integrated Nanotechnology (CINT), a U.S. Department of Energy, Office of Basic Energy Sciences user facility.

REFERENCES

(1) Fidler, A. F.; Singh, V. P.; Long, P. D.; Dahlberg, P. D.; Engel, G. S. Dynamic Localization of Electronic Excitations in Photosynthetic Complexes Revealed with Chiral Two-Dimensional Spectroscopy. *Nat. Commun.* **2014**, *5*, 3286.

(2) Scholes, G. D.; Fleming, G. R. On the Mechanism of Light Harvesting in Photosynthetic Purple Bacteria: B800 to B850 Energy Transfer. *J. Phys. Chem. B* **2000**, *104*, 1854−1868.

(3) Lefler, K. M.; Kim, C. H.; Wu, Y. L.; Wasielewski, M. R. Self-Assembly of Supramolecular Light-Harvesting Arrays from Symmetric Perylene-3,4-dicarboximide Trefoils. *J. Phys. Chem. Lett.* **2014**, *5*, 1608−1615.

(4) Uetomo, A.; Kozaki, M.; Suzuki, S.; Yamanaka, K.; Ito, O.; Okada, K. Efficient Light-Harvesting Antenna with a Multi-Porphyrin Cascade. *J. Am. Chem. Soc.* **2011**, *133*, 13276−13279.

(5) Leishman, C. W.; McHale, J. L. Light-Harvesting Properties and Morphology of Porphyrin Nanostructures Depend on Ionic Species Inducing Aggregation. *J. Phys. Chem. C* **2015**, *119*, 28167−28181.

(6) Ishida, Y.; Shimada, T.; Masui, D.; Tachibana, H.; Inoue, H.; Takagi, S. Efficient Excited Energy Transfer Reaction in Clay/Porphyrin Complex Toward an Artificial Light-Harvesting System. *J. Am. Chem. Soc.* **2011**, *133*, 14280−14286.

(7) Ziessel, R.; Ulrich, G.; Haefele, A.; Harriman, A. An Artificial Light-Harvesting Array Constructed from Multiple Bodipy Dyes. *J. Am. Chem. Soc.* **2013**, *135*, 11330−11344.

(8) Lee, C. Y.; Farha, O. K.; Hong, B. J.; Sarjeant, A. A.; Nguyen, S. T.; Hupp, J. T. Light-Harvesting Metal-Organic Frameworks (MOFs): Efficient Strut-to-Strut Energy Transfer in Bodipy and Porphyrin-Based MOFs. *J. Am. Chem. Soc.* **2011**, *133*, 15858−15861.

(9) Johnson, J. M.; Chen, R.; Chen, X.; Moskun, A. C.; Zhang, X.; Hogen-Esch, T. E.; Bradforth, S. E. Investigation of Macrocyclic Polymers as Artificial Light Harvesters: Subpicosecond Energy Transfer in Poly(9,9-Dimethyl-2-Vinylfluorene). *J. Phys. Chem. B* **2008**, *112*, 16367−16381.

(10) Aggarwal, A. V.; Thiessen, A.; Idelson, A.; Kalle, D.; Würsch, D.; Stangl, T.; Steiner, F.; Jester, S.-S.; Vogelsang, J.; Höger, S.; et al. Fluctuating Exciton Localization in Giant π-Conjugated Spoked-Wheel Macrocycles. *Nat. Chem.* **2013**, *5*, 964−970.

(11) Swallen, S. F.; Kopelman, R.; Moore, J. S.; Devadoss, C. Dendrimer Photoantenna Supermolecules: Energetic Funnels, Exciton Hopping and Correlated Excimer Formation. *J. Mol. Struct.* **1999**, *485−486*, 585−597.

(12) Andrews, D. L. Light Harvesting in Dendrimer Materials: Designer Photophysics and Electrodynamics. *J. Mater. Res.* **2012**, *27*, 627−638.

(13) Bradshaw, D. S.; Andrews, D. L. Mechanisms of Light Energy Harvesting in Dendrimers and Hyperbranched Polymers. *Polymers* **2011**, *3*, 2053−2077.

(14) Bosman, A. W.; Janssen, H. M.; Meijer, E. W. About Dendrimers: Structure, Physical Properties, and Applications. *Chem. Rev.* **1999**, *99*, 1665−1688.

(15) Ostroumov, E. E.; Mulvaney, R. M.; Cogdell, R. J.; Scholes, G. D. Broadband 2D Electronic Spectroscopy Reveals a Carotenoid Dark State in Purple Bacteria. *Science* **2013**, *340*, 52−56.

(16) Bakulin, A. A.; Silva, C.; Vella, E. Ultrafast Spectroscopy with Photocurrent Detection: Watching Excitonic Optoelectronic Systems at Work. *J. Phys. Chem. Lett.* **2016**, *7*, 250−258.

(17) Soavi, G.; Scotognella, F.; Lanzani, G.; Cerullo, G. Ultrafast Photophysics of Single-Walled Carbon Nanotubes. *Adv. Opt. Mater.* **2016**, *4*, 1670−1688.

(18) Galindo, J. F.; Atas, E.; Altan, A.; Kuroda, D. G.; Fernandez-Alberti, S.; Tretiak, S.; Roitberg, A. E.; Kleiman, V. D. Dynamics of Energy Transfer in a Conjugated Dendrimer Driven by Ultrafast Localization of Excitations. *J. Am. Chem. Soc.* **2015**, *137*, 11637−11644.

(19) Bradforth, S. E.; Jimenez, R.; van Mourik, F.; van Grondelle, R.; Fleming, G. R. Excitation Transfer in the Core Light-Harvesting Complex (LH-1) of Rhodobacter sphaeroides: An Ultrafast Fluorescence Depolarization and Annihilation Study. *J. Phys. Chem.* **1995**, *99*, 16179−16191.

(20) Camacho, R.; Tubasum, S.; Southall, J.; Cogdell, R. J.; Sforazzini, G.; Anderson, H. L.; Pullerits, T.; Scheblykin, I. G. Fluorescence Polarization Measures Energy Funneling in Single Light-Harvesting Antennas - LH2 vs Conjugated Polymers. *Sci. Rep.* **2015**, *5*, 15080.

(21) Yong, C.-K.; Parkinson, P.; Kondratuk, D.; Chen, W.-H.; Stannard, A.; Summerfield, A.; Sprafke, J.; O'Sullivan, M.; Beton, P.; Anderson, H.; et al. Ultrafast Delocalization of Excitation in Synthetic Light-Harvesting Nanorings. *Chem. Sci.* **2015**, *6*, 181−189.

(22) Varnavski, O.; Samuel, I. D. W.; Palsson, L.-O.; Beavington, R.; Burn, P. L.; Goodson, T. Investigations of Excitation Energy Transfer and Intramolecular Interactions in a Nitrogen Corded Distrylbenzene Dendrimer System. *J. Chem. Phys.* **2002**, *116*, 8893.

(23) Schmid, S. A.; Yim, K. H.; Chang, M. H.; Zheng, Z.; Huck, W. T. S.; Friend, R. H.; Kim, J. S.; Herz, L. M. Polarization Anisotropy Dynamics for Thin Films of a Conjugated Polymer Aligned by Nanoimprinting. *Phys. Rev. B: Condens. Matter Mater. Phys.* **2008**, *77*, 115338.

(24) Dykstra, T. E.; Hennebicq, E.; Beljonne, D.; Gierschner, J.; Claudio, G.; Bittner, E. R.; Knoester, J.; Scholes, G. D. Conformational Disorder and Ultrafast Exciton Relaxation in PPV-family Conjugated Polymers. *J. Phys. Chem. B* **2009**, *113*, 656−667.

(25) Yamazaki, I.; Akimoto, S.; Yamazaki, T.; Sato, S.-I.; Sakata, Y. Oscillatory Exciton Transfer in Dithiaanthracenophane: Quantum Beat a Coherent Photochemical Process in Solution. *J. Phys. Chem. A* **2002**, *106*, 2122−2128.

(26) Zhu, F.; Galli, C.; Hochstrasser, R. M. The Real-Time Intramolecular Electronic Excitation Transfer Dynamics of 9′,9-Bifluorene and 2′,2-Binaphtyl in Solution. *J. Chem. Phys.* **1993**, *98*, 1042−1057.

(27) Newbloom, G. M.; Hoffmann, S. M.; West, A. F.; Gile, M. C.; Sista, P.; Cheung, H.-K. C.; Luscombe, C. K.; Pfaendtner, J.; Pozzo, L. D. Solvatochromism and Conformational Changes in Fully Dissolved Poly(3-Alkylthiophene)s. *Langmuir* **2015**, *31*, 458−468.

(28) Petrone, A.; Goings, J. J.; Li, X. Quantum Confinement Effects on Optical Transitions in Nanodiamonds Containing Nitrogen Vacancies. *Phys. Rev. B: Condens. Matter Mater. Phys.* **2016**, *94*, 165402.

(29) Müller, J. G.; Atas, E.; Tan, C.; Schanze, K. S.; Kleiman, V. D. The Role of Exciton Hopping and Direct Energy Transfer in the Efficient Quenching of Conjugated Polyelectrolytes. *J. Am. Chem. Soc.* **2006**, *128*, 4007−4016.

(30) Ikeda, T.; Lee, B.; Kurihara, S.; Tazuke, S.; Ito, S.; Yamamoto, M. Time-Resolved Observation of Excitation Hopping Between Two Identical Chromophores Attached to Both Ends of Alkanes. *J. Am. Chem. Soc.* **1988**, *110*, 8299−8304.

(31) Hestand, N. J.; Spano, F. C. The Effect of Chain Bending on the Photophysical Properties of Conjugated Polymers. *J. Phys. Chem. B* **2014**, *118*, 8352−8363.

(32) Nayyar, I. H.; Batista, E. R.; Tretiak, S.; Saxena, A.; Smith, D. L.; Martin, R. L. Role of Geometric Distortion and Polarization in Localizing Electronic Excitations in Conjugated Polymers. *J. Chem. Theory Comput.* **2013**, *9*, 1144−1154.

(33) Shi, T.; Li, H.; Tretiak, S.; Chernyak, V. Y. How Geometric Distortions Scatter Electronic Excitations in Conjugated Macromolecules. *J. Phys. Chem. Lett.* **2014**, *5*, 3946−3952.

(34) Becker, K.; Da Como, E.; Feldmann, J.; Scheliga, F.; Csanyi, E.; Tretiak, S.; Lupton, J. M. How Chromophore Shape Determines the Spectroscopy of Phenylene Vinylenes: Origin of Spectral Broadening

DOI: 10.1021/acs.jpclett.7b00790
J. Phys. Chem. Lett. 2017, 8, 3020−3031

in the Absence of Aggregation. *J. Phys. Chem. B* **2008**, *112*, 4859−4864.
(35) Van Averbeke, B.; Beljonne, D. Conformational Effects on Excitation Transport Along Conjugated Polymer Chains. *J. Phys. Chem. A* **2009**, *113*, 2677−2682.
(36) Nelson, T.; Fernandez-Alberti, S.; Roitberg, A. E.; Tretiak, S. Conformational Disorder in Energy Transfer: Beyond Förster Theory. *Phys. Chem. Chem. Phys.* **2013**, *15*, 9245−9256.
(37) Ondarse-Alvarez, D.; Komurlu, S.; Roitberg, A. E.; Pierdominici-Sottile, G.; Tretiak, S.; Fernandez-Alberti, S.; Kleiman, V. D. Ultrafast Electronic Energy Relaxation in a Conjugated Dendrimer Leading to Inter-Branch Energy Redistribution. *Phys. Chem. Chem. Phys.* **2016**, *18*, 25080−25089.
(38) Ondarse-Alvarez, D.; Oldani, N.; Tretiak, S.; Fernandez-Alberti, S. Computational Study of Photoexcited Dynamics in Bichromophoric Cross-Shaped Oligofluorene. *J. Phys. Chem. A* **2014**, *118*, 10742−10753.
(39) Nguyen, T.-Q.; Martini, I. B.; Liu, J.; Schwartz, B. J. Controlling Interchain Interactions in Conjugated Polymers: The Effects of Chain Morphology on Exciton-Exciton Annihilation and Aggregation in MEH-PPV Films. *J. Phys. Chem. B* **2000**, *104*, 237−255.
(40) Barbatti, M. Nonadiabatic Dynamics with Trajectory Surface Hopping Method. *Wiley Interdiscip. Rev. Comput. Mol. Sci.* **2011**, *1*, 620−633.
(41) Wang, L.; Akimov, A.; Prezhdo, O. V. Recent Progress in Surface Hopping: 2011−2015. *J. Phys. Chem. Lett.* **2016**, *7*, 2100−2112.
(42) White, A.; Tretiak, S.; Mozyrsky, D. Coupled Wave-Packets for Non-Adiabatic Molecular Dynamics: A Generalization of Gaussian Wave-Packet Dynamics to Multiple Potential Energy Surfaces. *Chem. Sci.* **2016**, *7*, 4905−4911.
(43) Subotnik, J. E.; Jain, A.; Landry, B.; Petit, A.; Ouyang, W.; Bellonzi, N. Understanding the Surface Hopping View of Electronic Transitions and Decoherence. *Annu. Rev. Phys. Chem.* **2016**, *67*, 387−417.
(44) Zhu, C.; Nangia, S.; Jasper, A. W.; Truhlar, D. G. Coherent Switching with Decay of Mixing: An Improved Treatment of Electronic Coherence for Non-Born Oppenheimer Trajectories. *J. Chem. Phys.* **2004**, *121*, 7658−7670.
(45) Martens, C. C. Surface Hopping by Consensus. *J. Phys. Chem. Lett.* **2016**, *7*, 2610−2615.
(46) Richter, M.; Marquetand, P.; González-Vázquez, J.; Sola, I.; González, L. SHARC: ab Initio Molecular Dynamics with Surface Hopping in the Adiabatic Representation Including Arbitrary Couplings. *J. Chem. Theory Comput.* **2011**, *7*, 1253−1258.
(47) Granucci, G.; Persico, M.; Spighi, G. Surface Hopping Trajectory Simulations with Spin-Orbit and Dynamical Couplings. *J. Chem. Phys.* **2012**, *137*, 22A501.
(48) Cui, G.; Thiel, W. Generalized Trajectory Surface-Hopping Method for Internal Conversion and Intersystem Crossing. *J. Chem. Phys.* **2014**, *141*, 124101.
(49) Barbatti, M.; Ruckenbauer, M.; Plasser, F.; Pittner, J.; Granucci, G.; Persico, M.; Lischka, H. Newton-X: A Surface-Hopping Program for Nonadiabatic Molecular Dynamics. *Wiley Interdiscip. Rev. Comput. Mol. Sci.* **2014**, *4*, 26−33.
(50) Curchod, B. F. E.; Rauer, C.; Marquetand, P.; González, L.; Martínez, T. J. Communication: GAIMS—Generalized Ab Initio Multiple Spawning for Both Internal Conversion and Intersystem Crossing Processes. *J. Chem. Phys.* **2016**, *144*, 101102.
(51) Ishida, T.; Nanbu, S.; Nakamura, H. Clarification of Non-adiabatic Chemical Dynamics by the Zhu-Nakamura Theory of Nonadiabatic Transition: From Tri-Atomic Systems to Reactions in Solutions. *Int. Rev. Phys. Chem.* **2017**, *36*, 229−286.
(52) Tully, J. Molecular Dynamics with Electronic Transitions. *J. Chem. Phys.* **1990**, *93*, 1061−1071.
(53) Soler, M. A.; Roitberg, A. E.; Nelson, T.; Tretiak, S.; Fernandez-Alberti, S. Analysis of State-Specific Vibrations Coupled to the Unidirectional Energy Transfer in Conjugated Dendrimers. *J. Phys. Chem. A* **2012**, *116*, 9802−9810.
(54) Soler, M. A.; Nelson, T.; Roitberg, A. E.; Tretiak, S.; Fernandez-Alberti, S. Signature of Nonadiabatic Coupling in Excited-State Vibrational Modes. *J. Phys. Chem. A* **2014**, *118*, 10372−10379.
(55) Shenai, P. M.; Fernandez-Alberti, S.; Bricker, W. P.; Tretiak, S.; Zhao, Y. Internal Conversion and Vibrational Energy Redistribution in Chlorophyll A. *J. Phys. Chem. B* **2016**, *120*, 49−58.
(56) Paterlini, M.; Ferguson, D. Constant Temperature Simulations using the Langevin Equation with Velocity Verlet Integration. *Chem. Phys.* **1998**, *236*, 243−252.
(57) Attard, P. Statistical Mechanical Theory for Non-Equilibrium Systems. IX. Stochastic Molecular Dynamics. *J. Chem. Phys.* **2009**, *130*, 194113.
(58) Tretiak, S.; Chernyak, V.; Mukamel, S. Two-Dimensional Real-Space Analysis of Optical Excitations in Acceptor-Substituted Carotenoids. *J. Am. Chem. Soc.* **1997**, *119*, 11408−11419.
(59) Tretiak, S.; Chernyak, V.; Mukamel, S. Collective Electronic Oscillators for Nonlinear Optical Response of Conjugated Molecules. *Chem. Phys. Lett.* **1996**, *259*, 55−61.
(60) Stewart, J. J. P. Optimization of Parameters for Semiempirical Methods.I. Method. *J. Comput. Chem.* **1989**, *10*, 209−220.
(61) Stewart, J. J. P. Optimization of Parameters for Semiempirical Methods. II. Applications. *J. Comput. Chem.* **1989**, *10*, 221−264.
(62) Hernandez, L. A.; Nelson, T.; Tretiak, S.; Fernandez-Alberti, S. Photoexcited Energy Transfer in a Weakly Coupled Dimer. *J. Phys. Chem. B* **2015**, *119*, 7242−7252.
(63) Alfonso Hernandez, L.; Nelson, T.; Gelin, M. F.; Lupton, J. M.; Tretiak, S.; Fernandez-Alberti, S. Interference of Interchromophoric Energy-Transfer Pathways in π-Conjugated Macrocycles. *J. Phys. Chem. Lett.* **2016**, *7*, 4936−4944.
(64) Nelson, T.; Fernandez-Alberti, S.; Chernyak, V.; Roitberg, A. E.; Tretiak, S. Nonadiabatic Excited-State Molecular Dynamics Modeling of Photoinduced Dynamics in Conjugated Molecules. *J. Phys. Chem. B* **2011**, *115*, 5402−5414.
(65) Nelson, T.; Fernandez-Alberti, S.; Chernyak, V.; Roitberg, A.; Tretiak, S. Nonadiabatic Excited-State Molecular Dynamics: Numerical Tests of Convergence and Parameters. *J. Chem. Phys.* **2012**, *136*, 054108.
(66) Fernandez-Alberti, S.; Roitberg, A.; Nelson, T.; Tretiak, S. Identification of Unavoided Crossings in Nonadiabatic Photoexcited Dynamics Involving Multiple Electronic States in Polyatomic Conjugated Molecules. *J. Chem. Phys.* **2012**, *137*, 014512.
(67) Nelson, T.; Fernandez-Alberti, S.; Roitberg, A. E.; Tretiak, S. Nonadiabatic Excited-State Molecular Dynamics: Treatment of Electronic Decoherence. *J. Chem. Phys.* **2013**, *138*, 224111.
(68) Nelson, T.; Fernandez-Alberti, S.; Roitberg, A. E.; Tretiak, S. Nonadiabatic Excited-State Molecular Dynamics: Modeling Photophysics in Organic Conjugated Materials. *Acc. Chem. Res.* **2014**, *47*, 1155−1164.
(69) Fernandez-Alberti, S.; Roitberg, A. E.; Kleiman, V. D.; Nelson, T.; Tretiak, S. Shishiodoshi Unidirectional Energy Transfer Mechanism in Phenylene Ethynylene Dendrimers. *J. Chem. Phys.* **2012**, *137*, 22A526.
(70) Franklin-Mergarejo, R.; Alvarez, D. O.; Tretiak, S.; Fernandez-Alberti, S. Carbon Nanorings with Inserted Acenes: Breaking Symmetry in Excited State Dynamics. *Sci. Rep.* **2016**, *6*, 31253.
(71) Bricker, W. P.; Shenai, P. M.; Ghosh, A.; Liu, Z.; Grace, M.; Enriquez, M.; Lambrev, P. H.; Tan, H.-S.; Lo, C. S.; Tretiak, S.; et al. Non-radiative Relaxation of Photoexcited Chlorophylls: Theoretical and Experimental Study. *Sci. Rep.* **2015**, *5*, 13625.
(72) Clark, J.; Nelson, T.; Tretiak, S.; Cirmi, G.; Lanzani, G. Femtosecond Torsional Relaxation. *Nat. Phys.* **2012**, *8*, 225−231.
(73) Nelson, T.; Naumov, A.; Fernandez-Alberti, S.; Tretiak, S. Nonadiabatic Excited-State Molecular Dynamics: On-the-fly Limiting of Essential Excited States. *Chem. Phys.* **2016**, *481*, 84−90.
(74) Nelson, T.; Fernandez-Alberti, S.; Roitberg, A. E.; Tretiak, S. Artifacts Due to Trivial Unavoided Crossings in the Modeling of Photoinduced Energy Transfer Dynamics in Extended Conjugated Molecules. *Chem. Phys. Lett.* **2013**, *590*, 208−213.

DOI: 10.1021/acs.jpclett.7b00790
J. Phys. Chem. Lett. 2017, 8, 3020−3031

(75) Wang, L.; Prezhdo, O. V. A Simple Solution to the Trivial Crossing Problem in Surface Hopping. *J. Phys. Chem. Lett.* **2014**, *5*, 713−719.
(76) Meek, G. A.; Levine, B. G. Evaluation of the Time-Derivative Coupling for Accurate Electronic State Transition Probabilities from Numerical Simulations. *J. Phys. Chem. Lett.* **2014**, *5*, 2351−2356.
(77) Jain, A.; Alguire, E.; Subotnik, J. E. An Efficient, Augmented Surface Hopping Algorithm that Includes Decoherence for Use in Large-Scale Simulations. *J. Chem. Theory Comput.* **2016**, *12*, 5256−5268.
(78) Jaeger, H. M.; Fischer, S.; Prezhdo, O. V. Decoherence-Induced Surface Hopping. *J. Chem. Phys.* **2012**, *137*, 22A545.
(79) Granucci, G.; Persico, M.; Zoccante, A. Including Quantum Decoherence in Surface Hopping. *J. Chem. Phys.* **2010**, *133*, 134111.
(80) Subotnik, J. E. Fewest-Switches Surface Hopping and Decoherence in Multiple Dimensions. *J. Phys. Chem. A* **2011**, *115*, 12083−12096.
(81) Herman, M. F. Toward an Accurate and Efficient Semiclassical Surface Hopping Procedure for Nonadiabatic Problems. *J. Phys. Chem. A* **2005**, *109*, 9196−9205.
(82) Miller, W. H. The Semiclassical Initial Value Representation: A Potentially Practical Way for Adding Quantum Effects to Classical Molecular Dynamics Simulations. *J. Phys. Chem. A* **2001**, *105*, 2942−2955.
(83) Miller, W. H. Electronically Nonadiabatic Dynamics via Semiclassical Initial Value Methods. *J. Phys. Chem. A* **2009**, *113*, 1405−1415.
(84) Ben-Nun, M.; Quenneville, J.; Martínez, T. J. Ab Initio Multiple Spawning:? Photochemistry from First Principles Quantum Molecular Dynamics. *J. Phys. Chem. A* **2000**, *104*, 5161−5175.
(85) White, A. J.; Gorshkov, V. N.; Wang, R.; Tretiak, S.; Mozyrsky, D. Semiclassical Monte Carlo: A First Principles Approach to Non-Adiabatic Molecular Dynamics. *J. Chem. Phys.* **2014**, *141*, 184101.
(86) Kong, X.; Markmann, A.; Batista, V. S. Time-Sliced Thawed Gaussian Propagation Method for Simulations of Quantum Dynamics. *J. Phys. Chem. A* **2016**, *120*, 3260−3269.
(87) Tretiak, S.; Mukamel, S. Density Matrix Analysis and Simulation of Electronic Excitations in Conjugated and Aggregated Molecules. *Chem. Rev.* **2002**, *102*, 3171−3212.
(88) Mukamel, S.; Tretiak, S.; Wagersreiter, T.; Chernyak, V. Electronic Coherence and Collective Optical Excitations of Conjugated Molecules. *Science* **1997**, *277*, 781−787.
(89) Martin, R. L. Natural Transition Orbitals. *J. Chem. Phys.* **2003**, *118*, 4775−4777.
(90) Tretiak, S.; Isborn, C.; Niklasson, A.; Challacombe, M. Representation Independent Algorithms for Molecular Response Calculations in Time-Dependent Self-Consistent Field Theories. *J. Chem. Phys.* **2009**, *130*, 054111.
(91) Karabunarliev, S.; Baumgarten, M.; Bittner, E. R.; Mullen, K. Rigorous Franck Condon Absorption and Emission Spectra of Conjugated Oligomers from Quantum Chemistry. *J. Chem. Phys.* **2000**, *113*, 11372−11381.
(92) Gong, J. Q.; Favereau, L.; Anderson, H. L.; Herz, L. M. Breaking the Symmetry in Molecular Nanorings. *J. Phys. Chem. Lett.* **2016**, *7*, 332−338.
(93) Tommasini, M.; Chernyak, V.; Mukamel, S. Electronic Density-Matrix Algorithm for Nonadiabatic Couplings in Molecular Dynamics Simulations. *Int. J. Quantum Chem.* **2001**, *85*, 225−238.
(94) Mathew, S.; Yella, A.; Gao, P.; Humphry-Baker, R.; Curchod, B. F. E.; Ashari-Astani, N.; Tavernelli, I.; Rothlisberger, U.; Nazeeruddin, M. K.; Grätzel, M. Dye-Sensitized Solar Cells with 13% Efficiency Achieved Through the Molecular Engineering of Porphyrin Sensitizers. *Nat. Chem.* **2014**, *6*, 242−247.
(95) Landry, B. R.; Subotnik, J. E. Quantifying the Lifetime of Triplet Energy Transfer Processes in Organic Chromophores: A Case Study of 4-(2-Naphthylmethyl)Benzaldehyde. *J. Chem. Theory Comput.* **2014**, *10*, 4253−4263.
(96) Jaegermann, P.; Plato, M.; von Maltzan, B.; Mobius, K. Time-Resolved EPR Study of Exciton Hopping in Porphyrin Dimers in Their Photoexcited Triplet State. *Mol. Phys.* **1993**, *78*, 1057−1074.
(97) Tero-Kubota, S.; Miyamoto, T.; Akiyama, K.; Ikegami, Y.; Mataka, S.; Tashiro, M. Coherent and Incoherent Hopping of Triplet Exciton in Quinoxaline-Annelated and Naphthalene-Annelated Dimers. *Chem. Phys. Lett.* **1996**, *249*, 314−318.
(98) Sung, J.; Kim, P.; Fimmel, B.; Wurthner, F.; Kim, D. Direct Observation of Ultrafast Coherent Exciton Dynamics in Helical π-Stacks of Self-Assembled Perylene Bisimides. *Nat. Commun.* **2015**, *6*, 8646.
(99) Yang, L.; Caprasecca, S.; Mennucci, B.; Jang, S. Theoretical Investigation of the Mechanism and Dynamics of Intramolecular Coherent Resonance Energy Transfer in Soft Molecules: A Case Study of Dithia-anthracenophane. *J. Am. Chem. Soc.* **2010**, *132*, 16911−16921.
(100) Sato, S.-I.; Nishimura, Y.; Sakata, Y.; Yamazaki, I. Coherent Control of Oscillatory Exciton Transfer in Dithia-1,5(3,3)-anthracenophane by a Phase-Locked Femtosecond Pulse Pair. *J. Phys. Chem. A* **2003**, *107*, 10019−10025.
(101) Adamska, L.; Nayyar, I.; Chen, H.; Swan, A. K.; Oldani, N.; Fernandez-Alberti, S.; Golder, M. R.; Jasti, R.; Doorn, S. K.; Tretiak, S. Self-Trapping of Excitons, Violation of Condon Approximation, and Efficient Fluorescence in Conjugated Cycloparaphenylenes. *Nano Lett.* **2014**, *14*, 6539−6546.
(102) Parkinson, P.; Kondratuk, D. V.; Menelaou, C.; Gong, J. Q.; Anderson, H. L.; Herz, L. M. Chromophores in Molecular Nanorings: When Is a Ring a Ring? *J. Phys. Chem. Lett.* **2014**, *5*, 4356−4361.
(103) Darzi, E. R.; Hirst, E. S.; Weber, C. D.; Zakharov, L. N.; Lonergan, M. C.; Jasti, R. Synthesis, Properties, and Design Principles of Donor-Acceptor Nanohoops. *ACS Cent. Sci.* **2015**, *1*, 335−342.
(104) Yousaf, M.; Lough, A. J.; Schott, E.; Koivisto, B. D. BODIPY-Phenylacetylene Macrocycle Motifs for Enhanced Light-Harvesting and Energy Transfer Applications. *RSC Adv.* **2015**, *5*, 57490−57492.
(105) Kilina, S. V.; Kilin, D. S.; Prezhdo, O. V. Breaking the Phonon Bottleneck in PbSe and CdSe Quantum Dots: Time-Domain Density Functional Theory of Charge Carrier Relaxation. *ACS Nano* **2009**, *3*, 93−99.
(106) Scholes, G. D.; Fleming, G. R.; Chen, L. X.; Aspuru-Guzik, A.; Buchleitner, A.; Coker, D. F.; Engel, G. S.; van Grondelle, R.; Ishizaki, A.; Jonas, D. M.; et al. Using Coherence to Enhance Function in Chemical and Biophysical Systems. *Nature* **2017**, *543*, 647−656.

DOI: 10.1021/acs.jpclett.7b00790
J. Phys. Chem. Lett. 2017, 8, 3020−3031